# Autophagy inhibition and microRNA-199a-5p upregulation in paclitaxel-resistant A549/T lung cancer cells

TIANJIAO ZENG[1*], MINGSHI XU[1*], WANLI ZHANG[1], XIAOFAN GU[1], FANGQING ZHAO[1], XUAN LIU[2] and XIONGWEN ZHANG[1]

[1]Shanghai Engineering Research Center of Molecular Therapeutics and New Drug Development, School of Chemistry and Molecular Engineering, East China Normal University, Shanghai 200062; [2]Institute of Interdisciplinary Integrative Medicine Research, Shanghai University of Traditional Chinese Medicine, Shanghai 201203, P.R. China

Received February 27, 2021; Accepted April 27, 2021

DOI: 10.3892/or.2021.8100

**Abstract.** Multidrug resistance (MDR) is one of the major reasons for the clinical failure of cancer chemotherapy. Autophagy activation serves a crucial role in MDR. However, the specific molecular mechanism linking autophagy with MDR remains unknown. The results of the present study demonstrated that autophagy was inhibited and microRNA (miR)-199a-5p levels were upregulated in MDR model lung cancer cells (A549/T and H1299/T) compared with those in the parental cell lines. Paclitaxel (PTX) treatment increased the expression levels of miR-199a-5p in parental lung cancer cells compared with those in PTX-untreated cells, and these expression levels were negatively correlated with PTX sensitivity of the cells. miR-199a-5p knockdown in A549/T cells induced autophagy and resensitized cells to multiple chemotherapeutic drugs including PTX, taxotere, topotecan, SN38, oxaliplatin and vinorelbine. By contrast, miR-199a-5p overexpression in A549 cells suppressed autophagy and desensitized cells to these chemotherapeutic drugs. Mechanistically, the results of the present study demonstrated that miR-199a-5p blocked autophagy by activating the PI3K/Akt/mTOR signaling pathway and inhibiting the protein expression of autophagy-related 5. Furthermore, p62 protein was identified as a direct target of miR-199a-5p; miR-199a-5p bound to p62 mRNA to decrease its mRNA and protein expression levels. In conclusion, the results of the present study suggested that miR-199a-5p may contribute to MDR development in lung cancer cells by inhibiting autophagy and targeting p62. The regulatory effect of miR-199a-5p on autophagy may provide novel insights for future multidrug-resistant lung cancer chemotherapy.

*Correspondence to:* Professor Xiongwen Zhang, Shanghai Engineering Research Center of Molecular Therapeutics and New Drug Development, School of Chemistry and Molecular Engineering, East China Normal University, 3663 North Zhongshan Road, Shanghai 200062, P.R. China
E-mail: xwzhang@sat.ecnu.edu.cn

Professor Xuan Liu, Institute of Interdisciplinary Integrative Medicine Research, Shanghai University of Traditional Chinese Medicine, Shanghai 201203, P.R. China
E-mail: xuanliu@shutcm.edu.cn

*Contributed equally

*Key words:* multidrug resistance, microRNA-199a-5p, lung cancer cells, autophagy, p62 protein

## Introduction

Multidrug resistance (MDR) is an innate or acquired ability of cancer cells to evade the effects of multiple chemotherapeutic drugs with various mechanisms (1). MDR is a major issue in cancer chemotherapy, but the detailed mechanisms of MDR are not completely understood (2). Generally, several mechanisms such as overexpression of various members of the ATP binding cassette (ABC) transport proteins, autophagy induction, apoptosis inhibition, enhanced DNA repair, cancer stem cell regulation, miRNA regulation, hypoxia induction and epigenetic regulation are considered to be the factors of MDR occurrence (2).

Autophagy is a complex cell behavior characterized by a lysosomal degradation pathway that degrades damaged or superfluous cell components into basic molecules (3,4). During autophagy, the cytosolic form of LC3 (LC3I) is conjugated to phosphatidylethanolamine to form LC3-phosphatidylethanolamine conjugate (LC3II), which is recruited to autophagosomal membranes (5). The conversion of LC3I to LC3II via phosphatidylethanolamine conjugation has been accepted as the gold standard for autophagosome formation (6), and since the amount of LC3II is associated with the number of autophagosomes, the ratio of LC3II/LC3I is considered to be a measurement of autophagy activity; a high LC3II/LC3I ratio indicates the activation of autophagy (7-10) Accumulating evidence suggests that autophagy activation serves a crucial role in MDR by preventing death from apoptosis, hypoxia and stress responses (11,12). For example, autophagy activation can protect breast cancer cells from apoptosis induced by Epirubicin and Adriamycin (13,14). However, autophagy inhibition can also desensitize cancer cells to anticancer drug treatment (15,16). To date, no previous

studies have clearly explained the role of autophagy in MDR occurrence; a deeper understanding of autophagy in MDR cells is needed for cancer therapeutic purposes.

MicroRNAs (miRNAs) are a class of small noncoding RNAs comprising 19-22 nucleotides that have been reported to serve important roles in autophagy regulation in MDR bladder and gastric cancer cells (17,18). Notably, miR-199a-5p is involved in autophagy and drug resistance in osteosarcoma cells (19). Previous studies have demonstrated the miR-199a-5p reverses drug resistance by targeting DNA damage-regulated autophagy modulator 1 to inhibit protective autophagy or by repressing the Wnt2-mediated autophagy signaling pathway in leukemia cells (20,21). However, the direct target and detailed mechanism of miR-199a-5p in autophagy regulation in multidrug-resistant lung cancer cells have not been clarified to date.

The present study aimed to investigate the association between autophagy and MDR development in multidrug-resistant A549/T cells, and to determine the role and mechanism of miR-199a-5p in autophagy regulation and reversal of MDR in lung cancer cells.

## Materials and methods

*Cell lines and cell culture*. Human kidney cell line 293T were cultured in DMEM (Thermo Fisher Scientific, Inc.) containing 10% fetal bovine serum (FBS; Biological Industries) and antibiotics (100 U/ml penicillin and 100 $\mu$g/ml streptomycin; Biological Industries) at 37˚C with 5% $CO_2$. Human lung carcinoma cell lines A549, H1299 and H661, and human lung adenocarcinoma cell lines H522 and H1944, and Paclitaxel (PTX)-selected ABCB1-overexperssing lung carcinoma cell line A549/T were cultured in RPMI-1640 medium (Thermo Fisher Scientific, Inc.) containing 10% FBS and antibiotics at 37˚C with 5% $CO_2$. The A549/T cell line was generously provided by Professor Liguang Lou (Shanghai Institute of Materia Medica, Chinese Academy of Sciences, Shanghai, China), and all other cell lines were obtained from the American Type Culture Collection.

*Induction of a PTX-resistant H1299 cell line*. The PTX-resistant H1299 cell line was established using increasing concentrations of PTX as previously described (22). Briefly, the $IC_{50}$ value of PTX in H1299 cells was determined by the Cell Counting Kit-8 (CCK-8) assay (GlpBio Technology, Inc.) as described below to be ~30 nM. H1299 cells were incubated with 15 nM PTX (half of the corresponding $IC_{50}$) for 72 h, following which PTX was withdrawn and cells were cultured without PTX until cells recovered and tolerated for PTX at this concentration. The same process was repeated until the cells were resistant to the initial concentration; subsequently, the concentration of PTX doubled and gradually increased until a final concentration of 240 nM, and the protocol with each concentration was repeated twice. When the induced cells could survive in 240 nM, the cells were considered to be PTX-resistant and termed H1299/T cells.

*Cell Counting Kit-8 (CCK-8) assay*. To assess the sensitivity of cells to chemotherapeutic drugs, H1299, H1299/T, A549 and A549/T cells (untransfected and transfected) were plated in 96-well plates ($3.5x10^3$ cells/well) and allowed to attach overnight, and various concentrations of chemotherapeutic drugs PTX (0.3 to 3 $\mu$M for H1299 and H1299/T cells; 1 to 10 $\mu$M for A549/T cells; 0.01 to 100 nM for A549 cells), docetaxel (DOC; 1 nM to 3 $\mu$M for A549/T cells; 0.03 to 300 nM for A549 cells), topotecan (1 nM to 3 $\mu$M for A549/T cells; 0.0001 to 0.3 nM for A549 cells), SN38 (3 nM to 1 $\mu$M for A549/T cells; 0.01 to 300 nM for A549 cells), oxaliplatin (OXA; 3 nM to 10 $\mu$M for A549/T and A549 cells) and vinorelbine (NVB; 0.3 nM to 3 $\mu$M for A549/T cells; 0.01 to 3 nM for A549 cells) were added to the wells. Following a 72-h incubation, 10 $\mu$l/well CCK-8 reagent was added and incubated for an additional 1 h in a humidified atmosphere at 37˚C with 5% $CO_2$. The absorbance was measured at 450 nm using a SpectraMax M5 microplate reader (Molecular Devices, LLC). The inhibition rate was calculated using the following formula: Inhibition rate=$[(OD_{control\ cells}-OD_{treated\ cells})/OD_{control\ cells}]$ x100%. The $IC_{50}$ values were calculated using the survival curves (Fig. S4) by GraphPad Prism 5.0 software (GraphPad Software, Inc.) using at least eight concentrations for each cell line. The fold-resistance was calculated by dividing the $IC_{50}$ of drug-resistant cell lines by that obtained in the parent cell lines.

Cell proliferation was determined using CCK-8 assay as previously described (23). Briefly, A549 and A549/T cells (untransfected and transfected) were plated in 96-well plates ($1.5x10^3$ cells/well). Following incubation in a humidified atmosphere at 37˚C with 5% $CO_2$ for 24, 48 and 72 h, 10 $\mu$l CCK-8 reagent was added to each well and incubated for an additional 1 h in a humidified atmosphere at 37˚C with 5% $CO_2$, and absorbance at 450 nm was determined by SpectraMax M5 microplate reader (Molecular Devices, LLC.).

*Reverse transcription-quantitative (RT-q)PCR*. TRIzol® (Invitrogen; Thermo Fisher Scientific, Inc.) was used to extract total RNA from all cell lines according to the manufacturer's instructions. To obtain cDNA, 2 $\mu$g total RNA was reverse-transcribed using M-MLV RTase cDNA Synthesis Kit (Takara Biotechnology Co., Ltd.) according to the manufacturer's instructions at 42˚C for 60 min and 70˚C for 10 min, followed by 4˚C. qPCR was performed using the SYBR® Premix Ex Taq (Takara Biotechnology Co., Ltd.) on a CFX96 Real-Time PCR detection system (Bio-Rad Laboratories, Inc.). The thermocycling conditions were as follows: Pretreatment at 95˚C for 20 min, followed by 49 cycles at 95˚C for 10 sec, 59˚C for 20 sec and 72˚C for 10 sec, a melt curve at 65-95˚C with increments of 0.5˚C every 5 sec, and finally 4˚C for preservation. Specific PCR primers used in the present study were synthesized by Sangon Biotech Co., Ltd. and are listed in Table SI. For the detection of miRNA levels, RNU6-1 level was used as an internal reference for normalization, whereas β-actin levels were used as an internal reference for mRNAs. The relative expression was calculated by the $2^{-\Delta\Delta Cq}$ method (24).

*Neutral red staining*. Neutral red staining assay was performed to assess the quantity of the lysosome in cells. H1299, H1299/T, A549 and A549/T cells (untransfected and transfected) were plated in 6-well plates at the density of $5x10^4$ cells per well and allowed to attach overnight. Following treatment with chloroquine (CQ) for 24 h (25-27) or cultured with serum-free

medium (starvation) for 6 h, respectively, the cells were stained with neutral red stain solution (1:10 in 1X PBS) for 30 min in a humidified atmosphere at 37˚C with 5% $CO_2$. Images were captured by an Olympus IX3 fluorescence microscope (Olympus Corporation) in three or four fields per sample.

*miR-199a-5p knockdown (KD) and overexpression (OE).* The transfections of sh-miR-199a-5p into A549/T cells and miR-199a-5p into A549 cells were performed as previously described (23). The plasmids were designed with a GFP expression sequence to evaluate the success of the transfection. The miR-199a-5p shRNA coding sequence was cloned into pLV.I vector. The recombinant sh-miR-199a-5p plasmid was transfected into 293T cells ($5x10^5$ cells/well) along with pCMV-VSV-G, pMDLg/pRRE and pRSV-Rev using Lipofectamine™ 3000 (Invitrogen; Thermo Fisher Scientific, Inc.) to generate lentiviral supernatants containing the miR-199a-5p shRNA sequence. Different concentrations of plasmids were used, but the quantity of all plasmids was 3 $\mu$g, and the transfection duration was 48 h. Subsequently, the lentivirus supernatants (2 ml/well) were transduced into A549/T cells following ultrafiltration at 37˚C for 24 h, and puromycin (10 $\mu$g/ml) was used to select monoclonal miR-199a-5p-KD and vector control cells at 37˚C for 2 weeks. miR-199a-5p-OE cells were constructed using the same method; the miR-199a-5p coding sequence was cloned into a pLVGFP vector, and the recombinant miR-199a-5p plasmid was transfected into 293T cells along with pCMV-VSV-G, pMDLg/pRRE and pRSV-Rev using Lipofectamine® 3000 (Invitrogen; Thermo Fisher Scientific, Inc.) to generate lentiviral supernatants containing the miR-199a-5p coding sequence. The lentivirus supernatants (2 ml/well) were transduced into A549 cells following ultrafiltration at 37˚C for 24 h, and puromycin (10 $\mu$g/ml) was used to select monoclonal miR-199a-5p-OE and vector control cells at 37˚C for 2 weeks. The monoclonal miR-199a-5p-KD and vector control cells were termed A549/T-miR-199a-5p-KD and A549/T-pLV.I-vector, and the monoclonal miR-199a-5p-OE and vector control cells which were termed A549-miR-199a-5p-OE and A549-pGFP-vector, respectively.

*Western blotting.* Following various treatments, cells were lysed with RIPA buffer (Thermo Fisher Scientific, Inc.) and 100X phosphatase inhibitor cocktail (Thermo Fisher Scientific, Inc.). The protein concentration was determined using a BCA assay (Takara Biotechnology Co., Ltd.) and equalized prior to loading; a total of 20 $\mu$g of proteins were separated by 8-10% SDS-PAGE and transferred to a PVDF membrane. The membrane was blocked with 5% skimmed milk in PBS containing 0.1% Tween-800 (TPBS) for 1 h at room temperature and blotted with the relevant primary antibodies at 4˚C for 10-12 h, followed by incubation with HRP-conjugated secondary antibodies at room temperature for 1 h and visualization using the WB Femto ECL Substrate (CWBIO). β-Actin was used as the loading control. The primary antibodies used were as follows: LC3B (1:800; cat. no. 2775S), eukaryotic elongation factor 2 kinase (eEF2K; 1:1,000; cat. no. 3692S), PI3K (1:1,000; cat. no. 4263S), Akt (1:1,000; cat. no. 4691S), phosphor (p)-Akt (S473, D9E; 1:1,000; cat. no. 4060S), mTOR (7C10; cat. no. 2983S), p-mTOR (D9C2; 1:1,000; cat. no. 5536S)(all Cell Signaling Technology, Inc.), p62/SQSTM1 (1:2,500; cat. no. 18420-1-AP; Protein Tech Group, Inc.), autophagy-related 5 (ATG5; 1:1,000; cat. no. GTX113309; GeneTex, Inc.), ABCB1 (1:1,000; cat. no. P7965; MilliporeSigma) and β-Actin (1:5,000; cat. no. sc-1615; Santa Cruz Biotechnology, Inc).

*Dual-luciferase reporter assay.* Luciferase activity was measured using the Dual-Luciferase Reporter Assay system (Promega Corporation) according to the manufacturer's instructions. Briefly, A549-miR-199a-5p-OE and A549-pGFP-vector cells were plated in 96-well plates at the density of $3.5x10^3$ cells/well and allowed to attach overnight at 37˚C. psiCHECK-2 reporter plasmids (200 ng) containing the wild-type sequence which was 5'-GACACTTCG G-3' or mutated coding sequence which was 5'-GGGTGT GTCG-3' were transfected into the cells at 90% confluence. The wild-type sequence was obtained from the National Center for Biotechnology Information database (https://www.ncbi.nlm.nih.gov/gene/8878) and determined using Snapgene Software (GSL Biotech, LLC). Following 24-h transfection, the cells were lysed using the Passive Lysis Buffer from the Dual-Luciferase Reporter Assay system kit, and the luciferase activity was measured by a SpectraMax M5 Multi-Mode microplate reader (Molecular Devices, LLC). The firefly luciferase activity was normalized to that of *Renilla* luciferase, and the relative luciferase activity was calculated by dividing the luciferase activity value of the A549-miR-199a-5p-OE group by that obtained in vector group. The sequences used for plasmid sequencing were Rluc-Forward 5'-AGGACGCTC CAGATGAAATG-3' and psiCHECK-2-Reverse, 5'-ACTCAT TTAGATCCTCACAC-3'.

*MiRNA target gene prediction.* The target genes of miR-199a-5p were predicted using the online miRNA target prediction software TargetMiner (https://tools4mirs.org/software/target_prediction/targetminer/). The database analysis predicted 905 target genes of miR-199a-5p. Their binding to miR-199a-5p was compared, and the predicted genes were screened for those associated with autophagy. The identified targets were verified in A549-miR-199a-5p-OE and A549-pGFP-vector cells.

*Statistical analysis.* Data are presented as the mean ± SEM of three independent experiments. The statistical analysis was performed by GraphPad Prism software. Unpaired Student's t-test and one-way ANOVA with Dunnett's multiple comparison test were used to compare the samples. Pearson's correlation analysis was used to determine the relationships between continuous variables. $P<0.05$ was considered to indicate a statistically significant difference.

## Results

*Autophagy inhibition in drug-resistant A549/T and H1299/T lung cancer cells.* Four lung cancer cell lines were used in the present study, including the A549 and H1299 parental cell lines and PTX-resistant A549/T and H1299/T cells. The results of the CCK-8 assay demonstrated that the $IC_{50}$ values of A549/T and H1299/T cells were significantly higher compared with those of the parental cell lines (Table I).

Table I. Effects of paclitaxel on the $IC_{50}$ of A549, A549/T, H1299 and H1299/T cell lines.

| Cell line | $IC_{50}$, $\mu$M | Fold resistance | P-value[a] |
|---|---|---|---|
| A549 | 0.012±0.007 | 1.000 | |
| A549/T | 22.180±2.688 | 1,848.333 | <0.001 |
| H1299 | 0.030±0.013 | 1.000 | |
| H1299/T | 0.294±0.022 | 9.800 | <0.001 |

[a]Resistant vs. parental cells. Data are presented as the mean ± SEM from triplicate wells. The fold-resistance was calculated by dividing the $IC_{50}$ of multidrug-resistant cell lines by that obtained in parent cell lines.

To determine the association between autophagy and MDR, the protein expression levels of LC3I and LC3II were detected by western blotting. As presented in Fig. 1A, LC3I accumulated in A549/T cells, and the LC3II/LC3I ratio was lower compared with that in A549 cells following CQ treatment. Similar results were observed in the H1299/T cell line (Fig. 1B). Additionally, neutral red staining was used to determine intracellular lysosome formation. Neutral red accumulates in acidic vesicle organelles and is used for staining lysosomes and as an indicator of autophagy (27). As demonstrated in Fig. 1C, compared with A549/T cells, A549 cells displayed a higher number of red dots in the cytoplasm. Following CQ treatment and serum-free culture (6 h starvation), A549 cells exhibited higher accumulation of lysosomes with red staining compared with that in A549/T cells, suggesting that A549 cells had a higher basal autophagy level compared with A549/T cells, and A549/T displayed a lower response of autophagy induction by starvation. Similar results were observed in H1299 and H1299/T cells, which confirmed that autophagy was inhibited in drug-resistant lung cancer cells compared with that in the parental cell lines. Next, the expression levels of autophagy-related proteins were determined in A549 and A549/T cells. The results demonstrated that the PI3K/Akt/mTOR signaling pathway-related proteins and eEF2K were highly expressed in A549/T cells. By contrast, the ATG5 and p62 expression levels was significantly attenuated in A549/T cells compared with those in the parental A549 cells (Fig. 1D). These results suggested that autophagy was suppressed in A549/T and H1299/T cells, and that negative regulation of autophagy may be involved in MDR in lung cancer cells.

*miR-199a-5p is upregulated in drug-resistant A549/T and H1299/T cells.* As aforementioned, miR-199a-5p is associated with MDR (19). To determine the effects of miR-199a-5p on MDR, the present study evaluated the expression levels of miR-199a-5p in four lung cancer cell lines by RT-qPCR. The expression levels of miR-199a-5p were significantly higher in A549/T and H1299/T cells compared with those in their parental cells (Fig. 2A and B). Notably, PTX treatment increased the expression levels of miR-199a-5p in A549 and H1299 cells with a tendency of dose- and time-dependence (Fig. 2C and D). In addition, the expression levels of miR-199a-5p and the $IC_{50}$ values of cells to PTX were determined in six lung cancer cell lines. As demonstrated in Fig. 2E-G, the expression levels of miR-199a-5p were positively correlated with the $IC_{50}$ value of PTX in these cell lines (R=0.8515; P=0.015). These results suggested that miR-199a-5p was upregulated in drug-resistant A549/T and H1299/T cells, miR-199a-5p upregulation was PTX-dependent in lung cancer cells, and the expression levels of miR-199a-5p were associated with the resistance of lung cancer cells to PTX treatment.

*Knockdown of miR-199a-5p reverses the resistance of A549/T cells to chemotherapeutic drugs, and overexpression of miR-199a-5p induces drug resistance in A549 cells.* To further investigate the involvement of miR-199a-5p in MDR, miR-199a-5p-KD A549/T and miR-199a-5p-OE A549 cell lines were established. The GFP fluorescence observed in the four transfected cell lines demonstrated that the plasmid transfection was successful (Fig. S1). miR-199a-5p expression levels were downregulated in A549/T-miR-199a-5p-KD cells upregulated in A549-miR-199a-5p-OE cells compared with those in the corresponding vector groups (Fig. 3A and B). The CCK-8 assay results demonstrated that A549/T-miR-199a-5p-KD cells were sensitive to PTX, DOC, SN38 and OXA, as indicated by the reduced cell viability following treatment compared with that in the vector-transfected cells (Fig. 3C; Table II), whereas A549-miR-199a-5p-OE cells exhibited lower sensitivity to PTX, DOC, OXA and NVB compared with that in the corresponding vector control group (Fig. 3D; Table II).

*miR-199a-5p contributes to MDR by suppressing autophagy.* To further determine the underlying mechanism of MDR regulation by miR-199a-5p, autophagy levels were assessed in A549/T-miR-199a-5p-KD and A549-miR-199a-5p-OE cells. Western blot analysis demonstrated that the LC3II/LC3I ratio in A549/T-miR-199a-5p-KD cells was increased compared with that in the corresponding vector group, whereas the LC3II/LC3I ratio in A549-miR-199a-5p-OE cells was markedly decreased compared with the vector group following CQ treatment (Fig. 4A). In addition, compared with that in the vector cells, lysosomal accumulation appeared to be increased in A549/T-miR-199a-5p-KD and decreased in A549-miR-199a-5p-OE cells, and this effect was more pronounced following CQ treatment and serum-free culture (Fig. 4B). Since the ABCB1 expression levels and the proliferation of A549/T-miR-199a-5p-KD and A549-miR-199a-5p-OE cells remained unchanged compared with those in the corresponding vector groups (Fig. S3A and B), these results suggested that miR-199a-5p-mediated drug resistance in lung cancer cells was independent of ABCB1 expression and cell proliferation, but mainly associated with autophagy inhibition.

*miR-199a-5p regulates autophagy via the PI3K/Akt/mTOR signaling pathway and autophagy-related proteins.* Western blotting experiment results demonstrated that overexpression of miR-199a-5p increased the expression levels of the PI3K/Akt/mTOR signaling pathway-related proteins and eEF2K, whereas knockdown of miR-199a-5p decreased the expression levels of these proteins compared with those in the corresponding vector groups (Fig. 4C). TargetMiner database analysis revealed that miR-199a-5p bound to the ATG5 (NM_004849) 3'-untranslated region, which suggested that ATG5 may be a target of miR-199a-5p (Fig. S2A). Further results

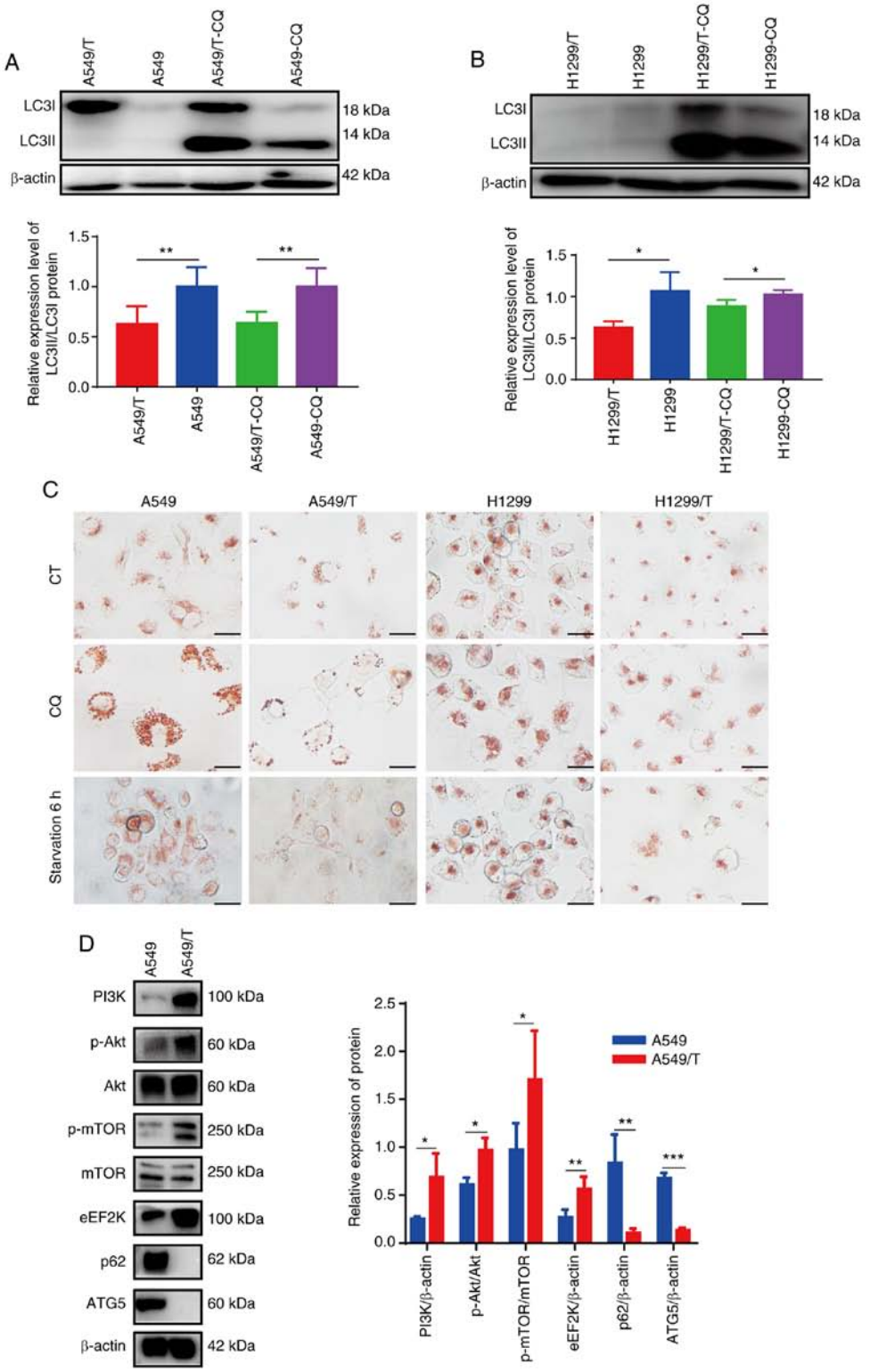


Figure 1. Autophagy inhibition in MDR A549/T and H1299/T cells. (A and B) Western blot analysis of LC3I and LC3II protein expression in cells treated with or without 10 $\mu$M CQ and the LC3II/LC3I ratio. β-actin was used as the loading control. (C) Neutral red staining for lysosomes analysis. Scale bar, 10 $\mu$m. (D) Western blot analysis of the expression levels of PI3K/Akt/mTOR pathway, eEF2K, p62 and ATG5 proteins, and the quantitative analysis results. The experiments were repeated three times, and representative bands are presented. $^{*}$P<0.05, $^{**}$P<0.01 and $^{***}$P<0.001. eEF2K, eukaryotic elongation factor 2 kinase; ATG5, autophagy-related 5; CQ, chloroquine; CT, control; p-, phosphorylated.

demonstrated that transfection with miR-199a-5p-OE attenuated ATG5 protein expression levels, whereas miR-199a-5p-KD did not affect ATG5 expression. RT-qPCR analysis revealed similar results: The mRNA expression levels of ATG5 were significantly downregulated in A549-miR-199a-5p-OE cells compared with those in the A549-pGFP-vector cells, but were not significantly increased in A549/T-miR-199a-5p-KD cells compared with those in the A549/T-pLV.I-vector cells (Fig. S2B). These results suggested that knockdown of miR-199a-5p induced autophagy, whereas overexpression of miR-199a-5p suppressed autophagy

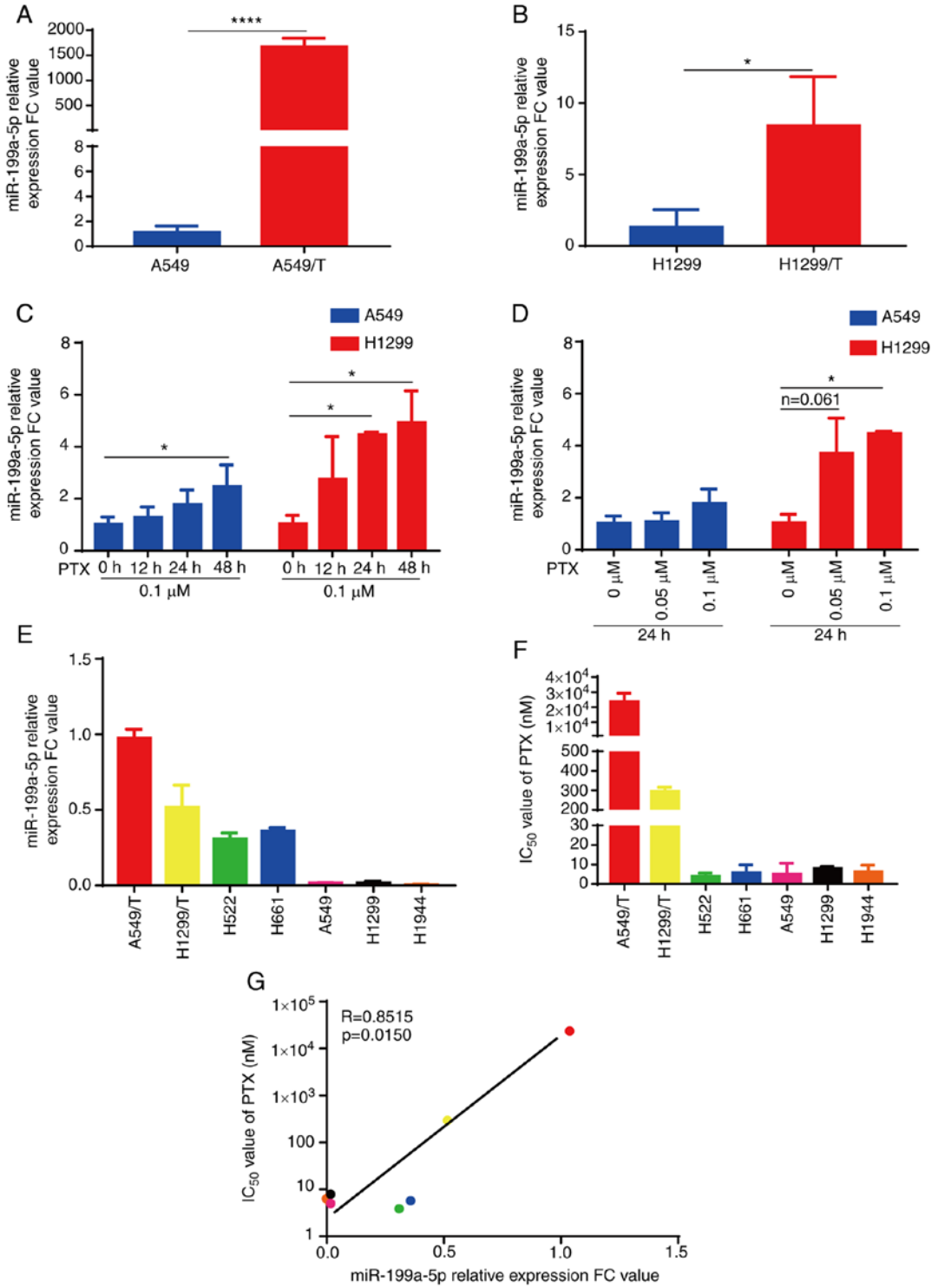


Figure 2. miR-199a-5p is upregulated in drug-resistant A549/T and H1299/T cells and associated with drug resistance. (A and B) RT-qPCR analysis of miR-199a-5p expression levels in (A) A549 and A549/T, and (B) H1299 and H1299/T lung cancer cell lines. (C and D) RT-qPCR analysis of miR-199a-5p expression levels in lung cancer cell lines treated with (C) 0.1 $\mu$M PTX for various times and (D) various concentrations of PTX for 24 h. (E) RT-qPCR analysis of miR-199a-5p expression levels in six lung cancer cell lines. (F) Cytotoxicity of PTX in seven lung cancer cell lines determined by the Cell Counting Kit-8 assay. (G) Correlation between drug sensitivity and miR-199a-5p expression levels in six lung cancer cell lines. $^{*}$P<0.05 and $^{****}$P<0.0001. miR, microRNA; RT-qPCR, reverse transcription-quantitative PCR; PTX, paclitaxel; FC, fold-change.

by activating PI3K/Akt/mTOR pathway and repressing ATG5 expression.

*miR-199a-5p targets p62*. The expression levels of p62 were significantly decreased in A549/T compared with those in the parental A549 cells (Fig. 1D) and in A549-miR-199a-5p-OE compared with those in the vector-transfected cells (Fig. 4C). In addition, knockdown of miR-199a-5p rescued the expression of p62 in A549/T cells (Fig. 4C). Therefore, we hypothesized that miR-199a-5p may directly target p62. Consistent with this hypothesis, analysis of the p62 coding sequence revealed six complementary bases paired with

Table II. Effects of miR-199a-5p on the sensitivity of cells to chemotherapeutic drugs.

| Drug | $IC_{50}$, $\mu$M | | | | $IC_{50}$, nM | | | |
|---|---|---|---|---|---|---|---|---|
| | A549/T-pLV.I-vector | A549/T-miR-199a-5p-KD | Fold-reversal | P-value | A549-pGFP-vector | A549-miR-199a-5p-OE | Fold-resistance | P-value |
| PTX | 1.776±0.078 | 0.295±0.053 | 6.020 | <0.001 | 0.267±0.147 | 0.897±0.107 | 3.340 | 0.011 |
| DOC | 0.194±0.047 | 0.062±0.010 | 3.129 | 0.015 | 0.220±0.072 | 0.686±0.256 | 3.118 | 0.039 |
| TPT | 0.096±0.010 | 0.071±0.016 | 1.352 | 0.083 | 0.047±0.005 | 0.107±0.030 | 2.277 | 0.076 |
| SN38 | 0.022±0.001 | 0.014±0.001 | 1.571 | 0.007 | 24.370±2.263 | 19.020±7.345 | 0.780 | 0.300 |
| OXA | 1.773±0.279 | 0.958±0.189 | 1.851 | 0.010 | 0.800±0.014[a] | 2.030±0.247 | 2.538 | 0.020 |
| NVB | 0.543±0.151 | 0.392±0.138 | 1.385 | 0.270 | 0.150±0.003 | 0.234±0.024 | 1.560 | 0.019 |

[a]The concentration of OXA in A549-pGFP-vector and A549-miR-199a-5p-OE cells are in $\mu$M. Data are presented as the mean ± SEM from triplicate wells. The fold-reversal was calculated by dividing the $IC_{50}$ of A549-pLV.I-vector cells by that in A549/T-miR-199a-5p-KD cells. The fold-resistance was calculated by dividing the $IC_{50}$ of A549-miR-199a-5p-OE cells by that obtained in A549-pGFP-vector cells. miR, microRNA; KD, knockdown; OE, overexpression; PTX, paclitaxel; DOC, docetaxel; TPT, topotecan; OXA, oxaliplatin; NVB, vinorelbine.

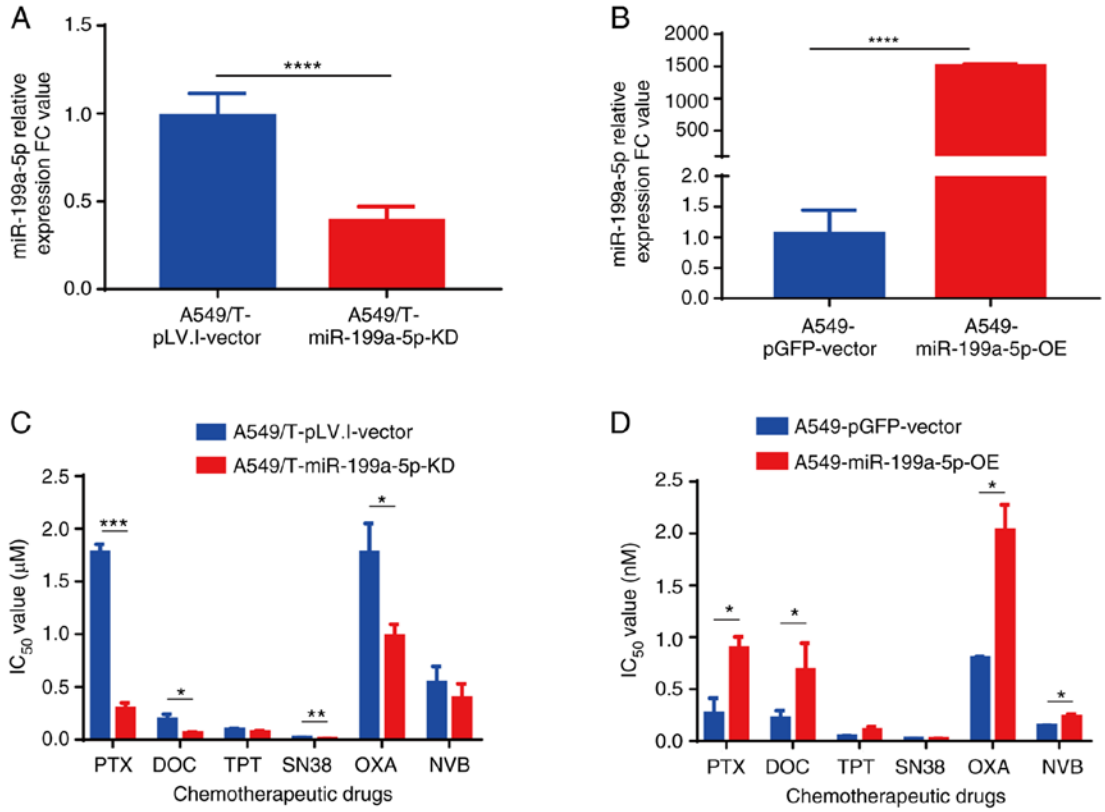


Figure 3. Knockdown and overexpression of miR-199a-5p affects cell sensitivity to chemotherapeutic drugs. (A and B) Reverse transcription-quantitative PCR analysis of miR-199a-5p expression levels in (A) A549/T-miR-199a-5p-KD and (B) A549-miR-199a-5p-OE cells. (C and D) The effects of various chemotherapeutic drugs on the viability of A549/T-miR-199a-5p-KD and A549-miR-199a-5p-OE cells determined by the Cell Counting Kit-8 assay. $^{*}$P<0.05, $^{**}$P<0.01, $^{***}$P<0.001 and $^{****}$P<0.0001. miR, microRNA; KD, knockdown; OE, overexpression; PTX, paclitaxel; DOC, docetaxel; TPT, topotecan; OXA, oxaliplatin; NVB, vinorelbine.

miR-199a-5p (Fig. 5A). Additionally, dual-luciferase reporter assay revealed that overexpression of miR-199a-5p reduced the luciferase activity of the p62 wild-type reporter compared with that in the mutated group, which confirmed that p62 was one of the direct targets of miR-199a-5p (Fig. 5B). In addition, overexpression of miR-199a-5p significantly downregulated, whereas knockdown of miR-199a-5p significantly upregulated the mRNA expression levels of p62 compared with those in the corresponding vector groups (Fig. 5C). Subsequently, the present study investigated the relationship between p62 protein (Fig. 5D) and miR-199a-5p (Fig. 2E) expression levels in six lung cancer cell lines. The results demonstrated that the protein expression levels of p62 were negatively correlated with miR-199a-5p expression levels in these lung cancer cell lines (R=-0.8545; P=0.0302) (Fig. 5E). These results suggested that p62 mRNA was a downstream target of

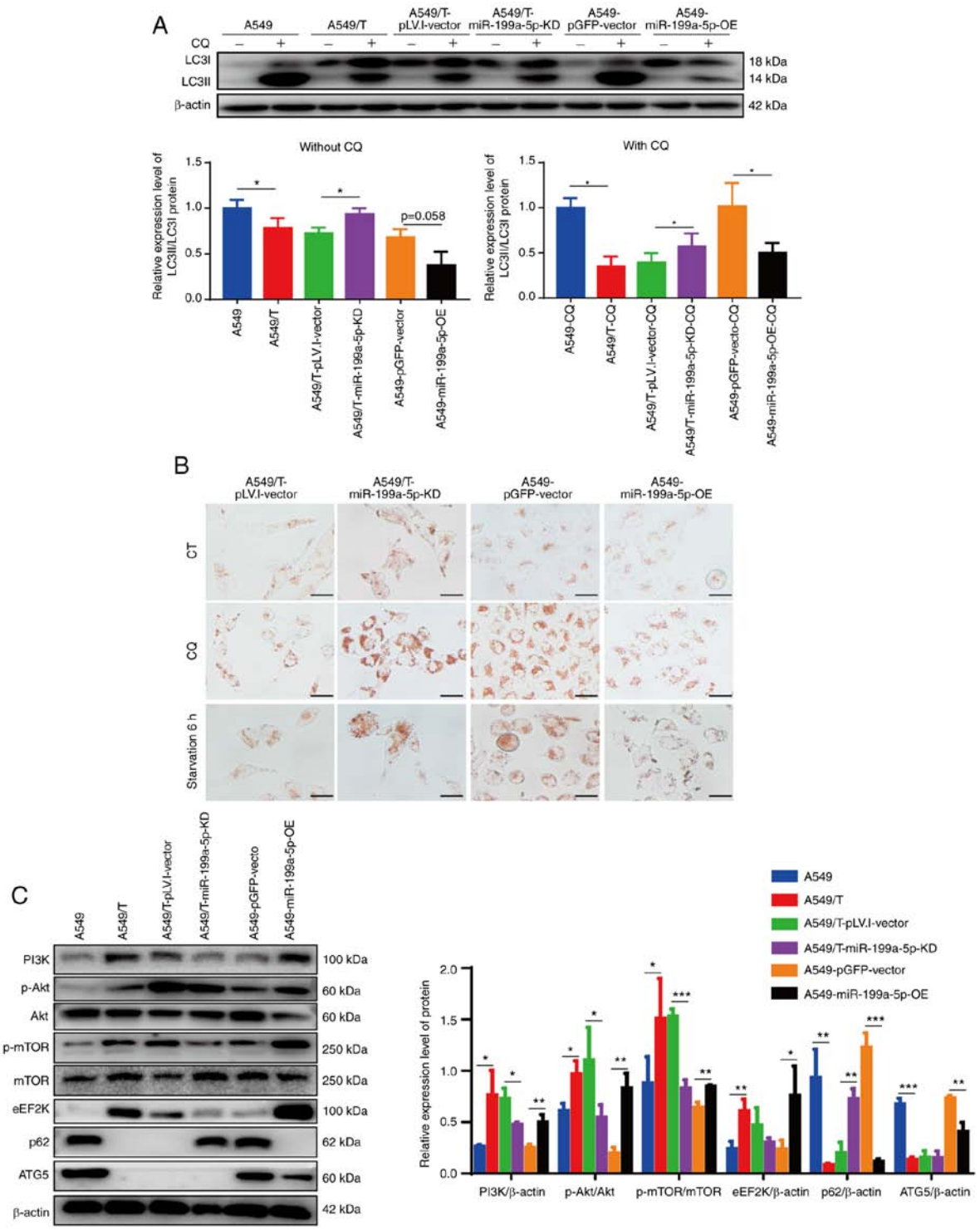


Figure 4. Knockdown and overexpression of miR-199a-5p affects cellular autophagy levels. (A) Western blot analysis of LC3I and LC3II protein expression levels in various cell lines and the LC3II/LC3I ratio with or without CQ treatment. β-actin was used as the loading control. (B) Neutral red staining for lysosome analysis. Scale bar, 10 $\mu$m. (C) Western blot analysis of the protein levels of PI3K/Akt/mTOR pathway, eEF2K, p62 and ATG5 proteins and the quantitative analysis results. The experiments were repeated three times and a representative data are presented. $^{*}$P<0.05, $^{**}$P<0.01 and $^{***}$P<0.001. miR, microRNA; KD, knockdown; OE, overexpression; eEF2K, eukaryotic elongation factor 2 kinase; ATG5, autophagy-related 5; CQ, chloroquine; CT, control; p-, phosphorylated.

miR-199a-5p, and that miR-199a-5p negatively regulated the levels of p62 protein.

## Discussion

Autophagy malfunction has been proposed to serve a crucial role in cancer development and resistance to chemotherapy (3). Autophagy activation may contribute to drug resistance (11,13,14) and may prevent cell death by apoptosis, necrosis or pyroptosis (28). Autophagy is crucial for reducing cellular stress (12), ROS production (11) and genomic instability (29), and direct evidence has demonstrated that autophagy activation regulates DNA damage response to capsaicin, which induces drug resistance (30).

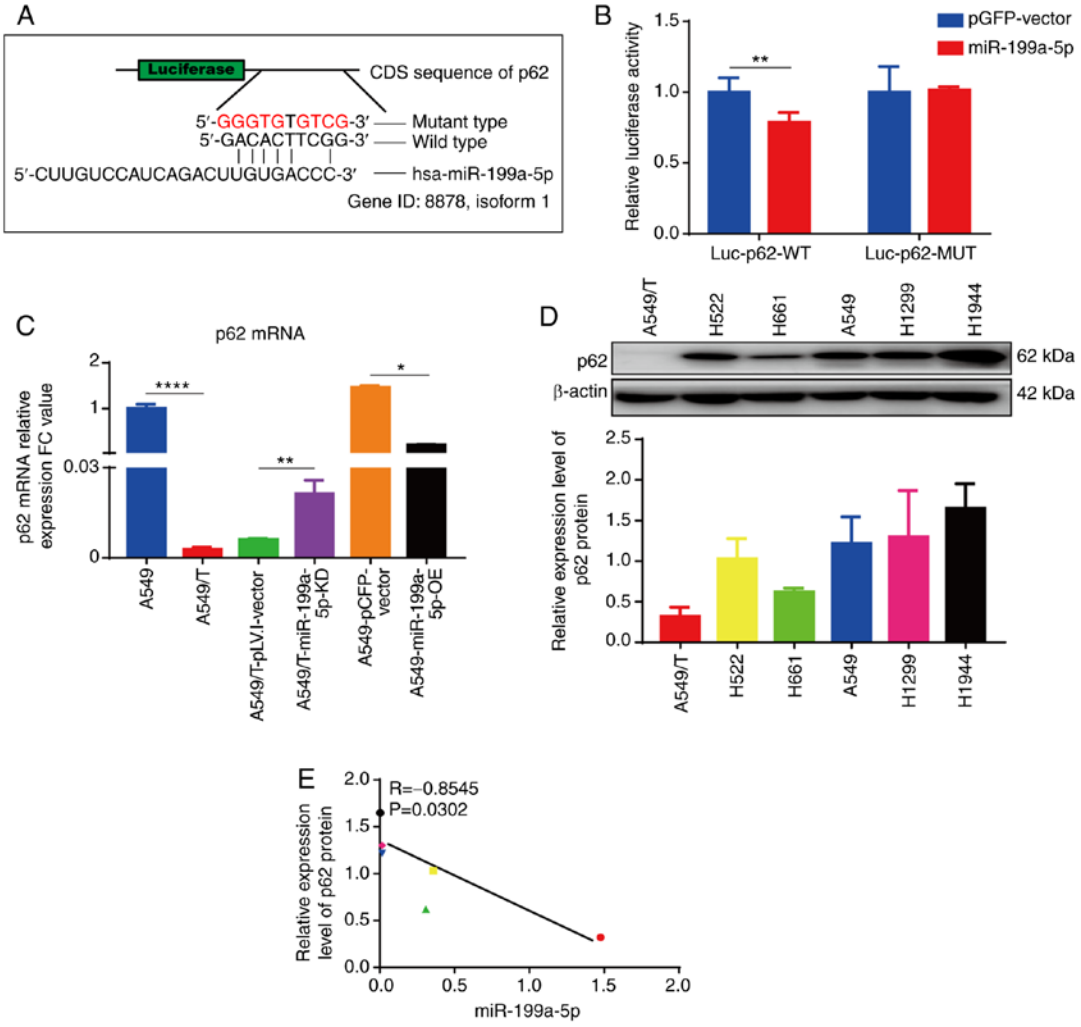


Figure 5. miR-199a-5p targets p62. (A) Putative target sites of miR-199a-5p in the coding sequence of p62. Red letters indicated the mutant luciferase reporter gene sequence of p62. (B) Effects of miR-199a-5p on p62 luciferase activity. (C) Reverse transcription-quantitative PCR analysis of the relative p62 mRNA expression levels in cells. (D) Western blot analysis of p62 protein expression levels in six lung cancer cell lines. (E) Correlation between the expression levels of miR-199a-5p and p62 protein in six lung cancer cell lines. The experiments were repeated three times, and representative data are presented. $^{*}$P<0.05, $^{**}$P<0.01 and $^{****}$P<0.0001. miR, microRNA; Luc-p62-WT, luciferase vector with a wild-type p62 sequence; Luc-p62-MUT, luciferase vector with a mutated p62 sequence.

In addition, as a prototypical damage-associated molecular pattern molecule, high-mobility group B1 is released following autophagy induction and promotes drug resistance in ovarian (31), colorectal (32) and lung (33) cancer. However, autophagy inhibition also affects MDR. For instance, Kanzawa *et al* (15) have reported that the autophagy inhibitor 3-MA suppresses the sequestration of cytoplasmic material during autophagy to rescue the tumor cells and promote resistance to chemotherapy. Lv *et al* (16) have demonstrated that curcumin decreases the levels of colon cancer-associated transcript 1 and sensitizes multidrug-resistant breast cancer cells to cisplatin via autophagy activation. Depending on the cell type, environment and stimulus, autophagy and cell death can have opposing, additive or even synergistic effects, which also leads to the development of drug resistance (34). In the present study, autophagy was inhibited in MDR lung cancer cells by miR-199a-5p overexpression, and the potential underlying mechanism included the activation of the PI3K/Akt/mTOR signaling pathway, upregulation of the protein expression levels of eEF2K and the attenuation of ATG5.

The activation of the PI3K/Akt/mTOR signaling pathway has been reported to induce the phosphorylation of ATG13 and block the initiation of autophagy (35). eEF2K is located downstream of the mTOR signaling pathway and is activated by phosphorylation of p70S6K to repress autophagy (35,36). By contrast, the suppression of eEF2K promotes autophagy (37,38) and enhances the cytotoxicity of fluoxetine in triple negative breast cancer cells (39). Therefore, high levels of eEF2K may inhibit autophagy and promote MDR in A549/T cells. In addition, ATG5 has been reported to serve an important role in the elongation and expansion of phagophore membrane; low levels of ATG5 lead to the failure of autophagosome maturation or inhibit the autophagy process, confirming its involvement in autophagy inhibition (4).

Previous studies have reported the downregulation of miR-199a-5p levels in drug-resistant cell lines compared with those in the corresponding parental cell lines (19-21). However, the present study was the first to reveal that the levels of miR-199a-5p were upregulated in MDR lung cancer cells compared with those in the parental cell lines. In the

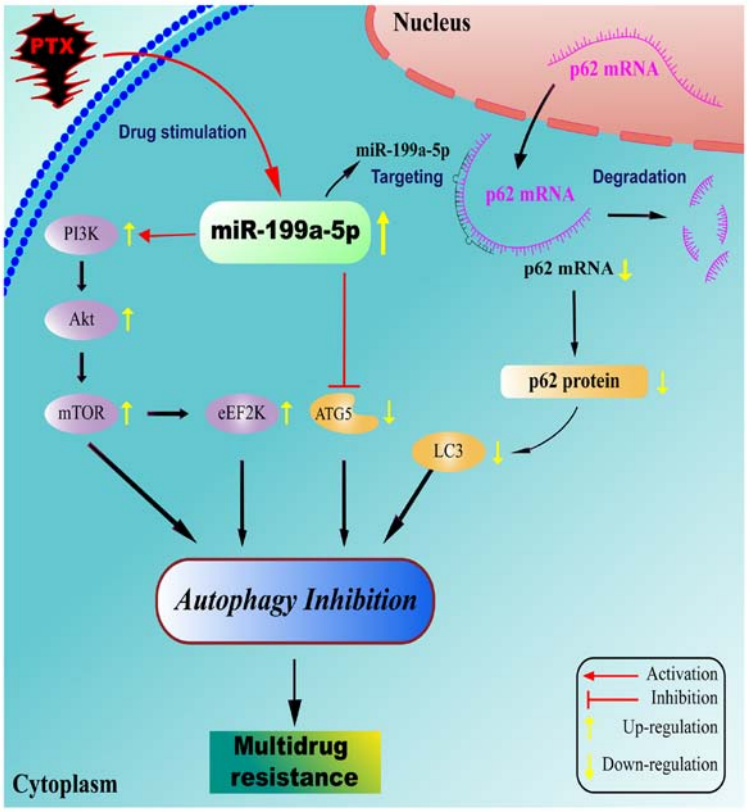


Figure 6. miR-199a-5p inhibits autophagy and targets p62 to desensitize tumor cells to chemotherapeutic drugs. PTX stimulation may enhance the expression levels of miR-199a-5p, which may activate the PI3K/Akt/mTOR pathway and induce eEF2K expression to negatively regulate autophagy initiation. Furthermore, elevation of miR-199a-5p may attenuate ATG5 expression and disrupt the elongation of autophagosome membrane to inhibit autophagy. In addition, miR-199a-5p may directly target p62 mRNA, leading to degradation and low p62 protein levels. The deficiency of p62 may inhibit autophagy by downregulating the LC3 protein levels to induce multidrug resistance. miR, microRNA; PTX, paclitaxel; eEF2K, eukaryotic elongation factor 2 kinase; ATG5, autophagy-related 5.

present study, RT-qPCR results demonstrated that the levels of miR-199a-5p were upregulated in PTX-resistant A549/T cells compared with those in the parental cells, which was different from imatinib-resistant K562, cisplatin-treated MG63 and Adriamycin-resistant K562 cells in previous studies (19-21). These results suggested that the effects of miR-199a-5p on MDR induction were cell line-specific. The upregulation of miR-199a-5p was negatively correlated with the sensitivity of lung cancer cells to PTX, indicating that the levels of miR-199a-5p may be used as a biomarker for the occurrence of MDR in lung cancer.

The knockdown of miR-199a-5p has been reported to result in the inhibition of pro-survival pathways, as observed by the downregulation of p-Akt, p-ERK and β-catenin protein levels in Huh7.5.1 cells infected with hepatitis C virus (40). Similarly, in the present study, miR-199a-5p-OE activated the PI3K/Akt/mTOR signaling pathway. In addition, the over-expression of miR-199a-5p increased the eEF2K expression levels compared with those in the control cells. Online miRNA target analysis software is normally used for target prediction (41,42). In the present study, TargetMiner database analysis revealed that ATG5 was a direct target of miR-199a-5p. The results of the validation assay demonstrated that the expression levels of ATG5 mRNA and protein were downregulated in A549-miR-199a-5p-OE cells compared with those in the vector-transfected cells, whereas A549/T-miR-199a-5p-KD cells exhibited no changes of ATG5 mRNA and protein levels, which suggested that miR-199a-5p may not be the only regulator of ATG5 (9). The activation of the PI3K/Akt/mTOR signaling pathway, enhancement of eEF2K and inhibition of ATG5 expression levels may be considered as the mechanism of autophagy suppression by miR-199a-5p in MDR A549/T cells (Fig. 6).

A notable result of the present study was that miR-199a-5p directly targeted p62, which led to the downregulation of p62 expression levels in autophagy-suppressed A549/T cells, which has not been investigated to date. Although miR-199a-5p may target other genes to induce MDR, p62 appears to be the major novel target of miR-199a-5p (43). p62 is considered to be a marker of autophagy; it accumulates in autophagy-suppressed cells, but does not participate in autophagy initiation (44). However, previous studies have suggested that p62 also serves a role in the autophagy process (43-45). Bjorkoy *et al* (45) have reported that the depletion of p62 inhibits the recruitment of LC3 to autophagosomes under starvation conditions, which indicates the accessibility for p62 in autophagy occurrence. In addition, the deficiency of p62 leads to impaired formation of LC3II and affect autophagy (46). Gao *et al* (47) have demonstrated that the 20S proteasome cleaves LC3 and disrupts the conjugation function of LC3 protein to further inhibit the autophagy process, whereas proteolysis of LC3 by the 20S proteasome is inhibited by p62. These findings suggest that p62 serves a positive role in autophagy activation, whereas the deficiency of p62 negatively affects the autophagy process (Fig. 6), which was different from the normal autophagy inhibition process (48,49). To the best of our knowledge, no

previous studies have reported the function of p62 in MDR development, and further research is needed.

In conclusion, the present study for the first time reported autophagy inhibition and miR-199a-5p upregulation in drug-resistant A549/T and H1299/T cells compared with those in their parental cells. The upregulation of miR-199a-5p expression levels was not only stimulated by PTX, but also negatively associated to the sensitivity of lung cancer cells to PTX. Knockdown of miR-199a-5p induced autophagy and resensitized cells to multiple chemotherapeutic drugs, whereas overexpression of miR-199a-5p suppressed autophagy and desensitized cells to multiple chemotherapeutic drugs. Activation of the PI3K/Akt/mTOR signaling pathway, increase in the levels of eEF2K and decrease in the ATG5 expression levels may be the potential mechanism to suppress autophagy and induce MDR. In addition, miR-199a-5p directly targeted p62 mRNA and reduced p62 expression levels. Deficiency of p62 might inhibit autophagy and induce MDR. Taken together, the results of the present study revealed a novel function of miR-199a-5p as an autophagy inhibitor and a promoter of MDR in lung cancer cells. The regulatory effects of miR-199a-5p on autophagy may provide a novel therapeutic strategy for future multidrug-resistant lung cancer therapy and drug development.

**Acknowledgements**

Paclitaxel-selected ATP-binding cassette B1-overexperssing lung carcinoma cell lines A549/T were generously provided by Professor Liguang Lou (Shanghai Institute of Materia Medica, Chinese Academy of Sciences, Shanghai, China).

**Funding**

This work was funded by The National Nature Science Foundation of China (grant nos. 81872496 and 81873056) and The Science and Technology Commission of Shanghai Municipality (grant nos. 20S11902200 and 16DZ2280100).

**Availability of data and materials**

All data generated or analyzed during this study are included in this published article.

**Authors' contributions**

XL, XZ and TZ conceived and designed the study. XZ and FZ analyzed the data. TZ and MX performed the experiments and wrote the manuscript. WZ, XG and FZ performed certain experiments. TZ, XL and XZ visualized the data and supervised the study. TZ, MX, WZ, XG, FZ, XL and XZ confirm the authenticity of all the raw data. All authors read and approved the final version of the manuscript.

**Ethics approval and consent to participate**

Not applicable.

**Patient consent for publication**

Not applicable.

**Competing interests**

The authors declare that they have no competing interests.

**References**

1. Alfarouk KO, Stock CM, Taylor S, Walsh M, Muddathir AK, Verduzco D, Bashir AH, Mohammed OY, Elhassan GO, Harguindey S, *et al*: Resistance to cancer chemotherapy: Failure in drug response from ADME to P-gp. Cancer Cell Int 15: 71, 2015.
2. Wu Q, Yang Z, Nie Y, Shi Y and Fan D: Multi-drug resistance in cancer chemotherapeutics: Mechanisms and lab approaches. Cancer Lett 347: 159-166, 2014.
3. Mizushima N, Levine B, Cuervo AM and Klionsky DJ: Autophagy fights disease through cellular self-digestion. Nature 451: 1069-1075, 2008.
4. Feng Y, He D, Yao Z and Klionsky DJ: The machinery of macro-autophagy. Cell Res 24: 24-41, 2014.
5. Tanida I, Ueno T and Kominami E: LC3 and autophagy. Methods Mol Biol 445: 77-88, 2008.
6. Runwal G, Stamatakou E, Siddiqi FH, Puri C, Zhu Y and Rubinsztein DC: LC3-positive structures are prominent in autophagy-deficient cells. Sci Rep 9: 10147, 2019.
7. Oh S, Xiaofei E, Ni D, Pirooz SD, Lee JY, Lee D, Zhao Z, Lee S, Lee H, Ku B, *et al*: Downregulation of autophagy by Bcl-2 promotes MCF7 breast cancer cell growth independent of its inhibition of apoptosis. Cell Death Differ 18: 452-464, 2011.
8. Yang J, Pi C and Wang G: Inhibition of PI3K/Akt/mTOR pathway by apigenin induces apoptosis and autophagy in hepatocellular carcinoma cells. Biomed Pharmacother 103: 699-707, 2018.
9. Tekirdag KA, Korkmaz G, Ozturk DG, Agami R and Gozuacik D: MIR181A regulates starvation- and rapamycin-induced autophagy through targeting of ATG5. Autophagy 9: 374-385, 2013.
10. Fang LM, Li B, Guan JJ, Xu HD, Shen GH, Gao QG and Qin ZH: Transcription factor EB is involved in autophagy-mediated chemoresistance to doxorubicin in human cancer cells. Acta Pharmacol Sin 38: 1305-1316, 2017.
11. Mishima Y, Terui Y, Mishima Y, Taniyama A, Kuniyoshi R, Takizawa T, Kimura S, Ozawa K and Hatake K: Autophagy and autophagic cell death are next targets for elimination of the resistance to tyrosine kinase inhibitors. Cancer Sci 99: 2200-2208, 2008.
12. Hu YL, Jahangiri A, Delay M and Aghi MK: Tumor cell autophagy as an adaptive response mediating resistance to treatments such as antiangiogenic therapy. Cancer Res 72: 4294-4299, 2012.
13. Sun WL, Chen J, Wang YP and Zheng H: Autophagy protects breast cancer cells from epirubicin-induced apoptosis and facilitates epirubicin-resistance development. Autophagy 7: 1035-1044, 2011.
14. Zhang P, Liu X, Li H, Chen Z, Yao X, Jin J and Ma X: TRPC5-induced autophagy promotes drug resistance in breast carcinoma via CaMKKβ/AMPKα/mTOR pathway. Sci Rep 7: 3158, 2017.
15. Kanzawa T, Germano IM, Komata T, Ito H, Kondo Y and Kondo S: Role of autophagy in temozolomide-induced cytotoxicity for malignant glioma cells. Cell Death Differ 11: 448-457, 2004.
16. Lv XA, Wang B, Xu XH, Lei P, Bin W, Dong XX, Zeng CH and Du QW: Curcumin re-sensitizes multidrug resistant (MDR) breast cancer to cisplatin through inducing autophagy by decreasing CCAT1 expression. RSC Adv 7: 33572-33579, 2017.
17. Wu J, Li W, Ning J, Yu W, Rao T and Cheng F: Long noncoding RNA UCA1 targets miR-582-5p and contributes to the progression and drug resistance of bladder cancer cells through ATG7-mediated autophagy inhibition. Onco Targets Ther 12: 495-508, 2019.
18. Chen S, Wu J, Jiao K, Wu Q, Ma J, Chen D, Kang J, Zhao G, Shi Y, Fan D and Zhao G: MicroRNA-495-3p inhibits multidrug resistance by modulating autophagy through GRP78/mTOR axis in gastric cancer. Cell Death Dis 9: 1070, 2018.
19. Li Y, Jiang W, Hu Y, Da Z, Zeng C, Tu M, Deng Z and Xiao W: MicroRNA-199a-5p inhibits cisplatin-induced drug resistance via inhibition of autophagy in osteosarcoma cells. Oncol Lett 12: 4203-4208, 2016.
20. Li Y, Zhang G, Wu B, Yang W and Liu Z: MiR-199a-5p represses protective autophagy and overcomes chemoresistance by directly targeting DRAM1 in acute myeloid leukemia. J Oncol 2019: 5613417, 2019.

21. Chen PH, Liu AJ, Ho KH, Chiu YT, Anne Lin ZH, Lee YT, Shih CM and Chen KC: MicroRNA-199a/b-5p enhance imatinib efficacy via repressing WNT2 signaling-mediated protective autophagy in imatinib-resistant chronic myeloid leukemia cells. Chem Biol Interact 291: 144-151, 2018.
22. Li Y, Li L, Guan Y, Liu X, Meng Q and Guo Q: MiR-92b regulates the cell growth, cisplatin chemosensitivity of A549 non small cell lung cancer cell line and target PTEN. Biochem Biophys Res Commun 440: 604-610, 2013.
23. Li Y, Chen L, Feng L, Zhu M, Shen Q, Fang Y, Liu X and Zhang X: NEK2 promotes proliferation, migration and tumor growth of gastric cancer cells via regulating KDM5B/H3K4me3. Am J Cancer Res 9: 2364-2378, 2019.
24. Livak KJ and Schmittgen TD: Analysis of relative gene expression data using real-time quantitative PCR and the 2(-Delta Delta C(T)) method. Methods 25: 402-408, 2001.
25. Mauthe M, Orhon I, Rocchi C, Zhou X, Luhr M, Hijlkema KJ, Coppes RP, Engedal N, Mari M and Reggiori F: Chloroquine inhibits autophagic flux by decreasing autophagosome-lysosome fusion. Autophagy 14: 1435-1455, 2018.
26. Moore CE, Wang X, Xie J, Pickford J, Barron J, Regufe da Mota S, Versele M and Proud CG: Elongation factor 2 kinase promotes cell survival by inhibiting protein synthesis without inducing autophagy. Cell Signal 28: 284-293, 2016.
27. Chen XL, Liu P, Zhu WL and Lou LG: DCZ5248, a novel dual inhibitor of Hsp90 and autophagy, exerts antitumor activity against colon cancer. Acta Pharmacol Sin 42: 132-141, 2021.
28. Duprez L, Wirawan E, Vanden Berghe T and Vandenabeele P: Major cell death pathways at a glance. Microbes Infect 11: 1050-1062, 2009.
29. Chang H and Zou Z: Targeting autophagy to overcome drug resistance: Further developments. J Hematol Oncol 13: 159, 2020.
30. Yoon JH, Ahn SG, Lee BH, Jung SH and Oh SH: Role of autophagy in chemoresistance: Regulation of the ATM-mediated DNA-damage signaling pathway through activation of DNA-PKcs and PARP-1. Biochem Pharmacol 83: 747-757, 2012.
31. Li S and Wei Y: Association of HMGB1, BRCA1 and P62 expression in ovarian cancer and chemotherapy sensitivity. Oncol Lett 15: 9572-9576, 2018.
32. Huang CY, Chiang SF, Chen WT, Ke TW, Chen TW, You YS, Lin CY, Chao KSC and Huang CY: HMGB1 promotes ERK-mediated mitochondrial Drp1 phosphorylation for chemoresistance through RAGE in colorectal cancer. Cell Death Dis 9: 1004, 2018.
33. Zheng H, Chen JN, Yu X, Jiang P, Yuan L, Shen HS, Zhao LH, Chen PF and Yang M: HMGB1 enhances drug resistance and promotes in vivo tumor growth of lung cancer cells. DNA Cell Biol 35: 622-627, 2016.
34. Wirawan E, Vanden Berghe T, Lippens S, Agostinis P and Vandenabeele P: Autophagy: For better or for worse. Cell Res 22: 43-61, 2012.
35. Xie T, Li SJ, Guo MR, Wu Y, Wang HY, Zhang K, Zhang X, Ouyang L and Liu J: Untangling knots between autophagic targets and candidate drugs, in cancer therapy. Cell Prolif 48: 119-139, 2015.
36. Wu H, Yang JM, Jin S, Zhang H and Hait WN: Elongation factor-2 kinase regulates autophagy in human glioblastoma cells. Cancer Res 66: 3015-3023, 2006.
37. Pan Z, Chen Y, Liu J, Jiang Q, Yang S, Guo L and He G: Design, synthesis, and biological evaluation of polo-like kinase 1/eukaryotic elongation factor 2 kinase (PLK1/EEF2K) dual inhibitors for regulating breast cancer cells apoptosis and autophagy. Eur J Med Chem 144: 517-528, 2018.
38. Xie CM, Liu XY, Sham KW, Lai JM and Cheng CH: Silencing of EEF2K (eukaryotic elongation factor-2 kinase) reveals AMPK-ULK1-dependent autophagy in colon cancer cells. Autophagy 10: 1495-1508, 2014.
39. Sun D, Zhu L, Zhao Y, Jiang Y, Chen L, Yu Y and Ouyang L: Fluoxetine induces autophagic cell death via eEF2K-AMPK-mTOR-ULK complex axis in triple negative breast cancer. Cell Prolif 51: e12402, 2018.
40. Wang H, Gao H, Duan S and Song X: Inhibition of microRNA-199a-5p reduces the replication of HCV via regulating the pro-survival pathway. Virus Res 208: 7-12, 2015.
41. Wang G, Sun D, Li W and Xin Y: AKNA is a potential prognostic biomarker in gastric cancer and function as a tumor suppressor by modulating EMT-related pathways. Biomed Res Int 2020: 6726759, 2020.
42. Murugesan M and Premkumar K: Integrative miRNA-mRNA functional analysis identifies miR-182 as a potential prognostic biomarker in breast cancer. Mol Omics: Apr 22, 2021 (Epub ahead of print). doi: 10.1039/d0mo00160k.
43. Zhang K, Zhang X, Cai Z, Zhou J, Cao R, Zhao Y, Chen Z, Wang D, Ruan W, Zhao Q, *et al*: A novel class of microRNA-recognition elements that function only within open reading frames. Nat Struct Mol Biol 25: 1019-1027, 2018.
44. Moscat J, Karin M and Diaz-Meco MT: p62 in cancer: Signaling adaptor beyond autophagy. Cell 167: 606-609, 2016.
45. Bjorkoy G, Lamark T, Brech A, Outzen H, Perander M, Overvatn A, Stenmark H and Johansen T: p62/SQSTM1 forms protein aggregates degraded by autophagy and has a protective effect on huntingtin-induced cell death. J Cell Biol 171: 603-614, 2005.
46. Peng H, Yang J, Li G, You Q, Han W, Li T, Gao D, Xie X, Lee BH, Du J, *et al*: Ubiquitylation of p62/sequestosome1 activates its autophagy receptor function and controls selective autophagy upon ubiquitin stress. Cell Res 27: 657-674, 2017.
47. Gao Z, Gammoh N, Wong PM, Erdjument-Bromage H, Tempst P and Jiang X: Processing of autophagic protein LC3 by the 20S proteasome. Autophagy 6: 126-137, 2010.
48. Bjørkøy G, Lamark T, Pankiv S, Øvervatn A, Brech A and Johansen T: Monitoring autophagic degradation of p62/SQSTM1. Methods Enzymol 452: 181-197, 2009.
49. Zhang CF, Gruber F, Ni C, Mildner M, Koenig U, Karner S, Barresi C, Rossiter H, Narzt MS, Nagelreiter IM, *et al*: Suppression of autophagy dysregulates the antioxidant response and causes premature senescence of melanocytes. J Invest Dermatol 135: 1348-1357, 2015.

This work is licensed under a Creative Commons Attribution-NonCommercial-NoDerivatives 4.0 International (CC BY-NC-ND 4.0) License.